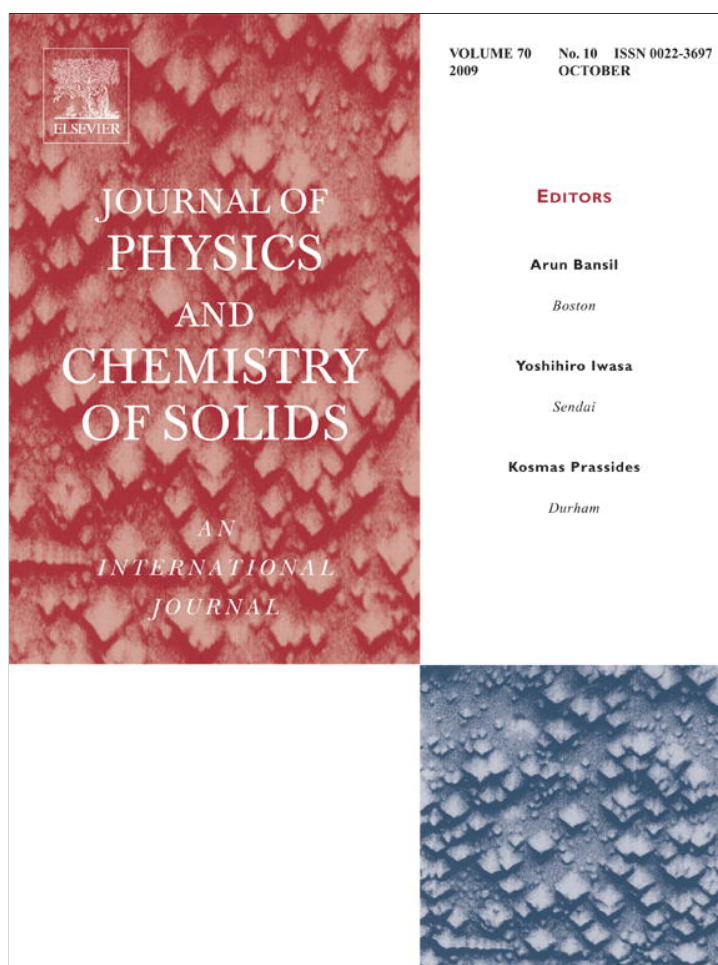


Provided for non-commercial research and education use.
Not for reproduction, distribution or commercial use.



This article appeared in a journal published by Elsevier. The attached copy is furnished to the author for internal non-commercial research and education use, including for instruction at the authors institution and sharing with colleagues.

Other uses, including reproduction and distribution, or selling or licensing copies, or posting to personal, institutional or third party websites are prohibited.

In most cases authors are permitted to post their version of the article (e.g. in Word or Tex form) to their personal website or institutional repository. Authors requiring further information regarding Elsevier's archiving and manuscript policies are encouraged to visit:

<http://www.elsevier.com/copyright>



Structure and electrical properties of SrO-borovanadate $(V_2O_5)_{0.5}(SrO)_{0.5-y}(B_2O_3)_y$ glasses

G.D. Khattak*, A. Mekki

Physics Department, King Fahd University of Petroleum & Minerals, Dhahran 31261, Saudi Arabia

ARTICLE INFO

Article history:

Received 18 December 2008

Received in revised form

4 May 2009

Accepted 29 June 2009

PACS:

61.10.Nz

61.14.Qp

61.43.Fs

61.82.Fk

71.23.Cq

72.15.Cz

Keywords:

D. Electrical conductivity

ABSTRACT

SrO-borovanadate glasses with nominal composition $(V_2O_5)_{0.5}(SrO)_{0.5-y}(B_2O_3)_y$, $0.0 \leq y \leq 0.4$ were prepared by a normal quench technique and investigated by direct current (DC) electrical conductivity, inductively coupled plasma (ICP) spectroscopy, infrared (IR) spectroscopy and X-ray powder diffraction (XRD) studies in an attempt to understand the nature of mechanism governing the DC electrical conductivity and the effect of addition of B_2O_3 on the structure and electrical properties of these glasses. XRD patterns confirm the amorphous nature of the present glasses and actual compositions of the glasses were determined by ICP spectroscopy. The temperature dependence of DC electrical conductivity of these glasses has been studied in terms of different hopping models. The IR results agree with previous investigations on similar glasses and it has been concluded that similar to SrO-vanadate glasses, metavanadate chain-like structures of SrV_2O_6 and individual VO_4 units also occur in SrO-borovanadate glasses. The SrV_2O_6 and VO_n polyhedra predominate in the low B_2O_3 -containing SrO-borovanadate glasses as B substitutes into the V sites of the various VO_n polyhedra and only when the concentration of B_2O_3 exceeds the SrO content do BO_n structures appear. This qualitative picture of three distinct structural groupings for Sr-vanadate and Sr-borovanadate glasses is consistent with the proposed glass structure on previous IR and extended X-ray absorption fine structure (EXAFS) studies on these types of glasses. The conductivity results were analyzed with reference to theoretical models existing in the literature and the analysis shows that the conductivity data are consistent with Mott's nearest neighbor hopping model. Analysis of the conductivity data shows that they are consistent with Mott's nearest neighbor hopping model. However, both Mott VRH and Greaves models are suitable to explain the data. Schnakenberg's generalized polaron hopping model is also consistent with temperature dependence of activation energy. However, various model parameters such as density of states, hopping energy, etc. obtained from the best fits were not found to be in accordance with the prediction of the Mott model.

© 2009 Elsevier Ltd. All rights reserved.

1. Introduction

Transition metal (TM) oxide glasses have been frequently studied from both mechanical and physical points of view in order to better understand the transport mechanism in these semiconducting glasses [1–3]. The semiconducting behavior in these glasses arises from an unpaired $3d^1$ electron hopping between TM ions [1,4,5] when the TM ions exist in two or more valence states, e.g., from an electron hopping from a V^{4+} site to a V^{5+} site. Since the unpaired electron induces a polarization around the TM ion, conduction can be described in terms of a model based on polarons. In recent years, amorphous V_2O_5 has attracted attention because of its potential use as a cathode material in solid-state devices. Direct current (DC) conductivity of vanadium oxide glasses in which V_2O_5 is associated with other glass formers such as TeO_2 , As_2O_3 , P_2O_5 has been extensively studied and these studies have shown that the

“small polaron” model can be used to describe the electronic transport phenomena in these materials. Several studies have been made on the structure of Sr and other vanadate glasses [6–9]. Very few studies have been carried out on glasses containing B_2O_3 and V_2O_5 . These glasses have their potential applications as optical and electrical memory switching [10], cathode materials for making solid devices and optical fiber [11,12]. In the present work, the effect of B_2O_3 content on the electrical and structural properties of SrO-borovanadate glasses has been examined with the help of Fourier transform infrared spectroscopy and DC conductivity studies as explained. It is hoped that this experimental data will help in further understanding the mechanisms of the electrical properties in these glasses.

2. Experimental methods

2.1. Sample preparation

The glasses investigated in this paper were prepared by melting dry mixtures of reagent-grade V_2O_5 , B_2O_3 and SrO in

* Corresponding author.

E-mail address: gkhattak@kfupm.edu.sa (G.D. Khattak).

Table 1

Nominal and actual molar compositions of Sr-borovanadate $(V_2O_5)_{0.5}(SrO)_{0.5-y}(B_2O_3)_y$ glasses.

Nominal	SrO	B ₂ O ₃	V ₂ O ₅	Al ₂ O ₃
y = 0.0	0.497	–	0.482	0.021
y = 0.1	0.373	0.0987	0.458	0.070
y = 0.2	0.284	0.179	0.448	0.090
y = 0.3	0.192	0.280	0.468	0.060
y = 0.4	0.092	0.384	0.454	0.070

The uncertainty in the ICP analysis of the molar fraction is $\pm 5\%$.

alumina crucibles with nominal compositions $(V_2O_5)_{0.5}(SrO)_{0.5-y}(B_2O_3)_y$, $0.0 \leq y \leq 0.4$. Since the oxidation and reduction reactions in a glass melt are known to depend on the size of the melt, on the sample geometry, on whether the melt is static or stirred, on thermal history and on quenching rate, all glass samples were prepared under similar conditions to standardize these factors. Approximately 30 g of chemicals were thoroughly mixed to obtain a homogenized mixture for each V₂O₅ concentration. The crucible containing the batch mixture was then transferred to an electrically heated melting furnace maintained at 1000–1100 °C depending on the composition of the sample. The melt was left for about an hour under atmospheric conditions in the furnace during which the melt was occasionally stirred with an alumina rod. The homogenized melt was then cast onto a stainless-steel plate mold to form glass disks of approximately 1.5 cm diameter and 3 mm thickness for DC conductivity measurements. After casting, the specimens were annealed at 200 °C for 2 h. X-ray powder diffraction patterns indicated that the glasses formed were completely amorphous. After preparation, the samples were stored in a vacuum desiccator to minimize any further oxidation of the glass samples. The actual compositions of glasses were determined by inductively coupled plasma spectroscopy (ICP) and are listed in Table 1. The inclusion of alumina from the crucibles used in melting of the glass mixtures is a possible source of impurities and has been detected in the ICP studies of these glasses.

2.2. Measurement techniques

2.2.1. DC conductivity

For measuring DC conductivity, disc-shaped samples were made, polished and then the evaporation of gold electrodes on polished surfaces was carried out in vacuum. Measurements of DC conductivity as a function of temperature, in all the samples, were made by the two-probe technique. A constant voltage was applied and the current was measured in the temperature range 293–473 K. To obtain the variation of conductivity with temperature, the sample was placed in a furnace, brought to the desired temperature and maintained at that temperature for sufficient time before taking the measurements to ensure thermal stability. The temperature was measured by a Pt/Pt–10% Rh thermocouple. From the conductivity versus temperature data, the values of different parameters were obtained using different theoretical models as explained in Section 4.

2.2.2. X-ray diffraction (XRD)

X-ray diffraction (XRD) patterns of the samples were recorded using a Shimadzu XRD-6000 X-ray diffractometer using a Cu anode (K_α , $\lambda = 1.5418 \text{ \AA}$).

2.2.3. Infrared spectra (IR)

Infrared spectra (IR) were recorded on a Perkin-Elmer Model 16F PC FT-IR spectrophotometer loaded with spectrum v2.00

software (MA, USA). Sample pellets for various glasses were prepared for FT-IR measurements by mixing approximately 1–2 mg the glass powder with about 100–150 mg of spectroscopic-grade KBr powder and grinding the mixture to a very fine powder and then compressing the mixture in an evacuable die under 10,000 pound pressure. The KBr powder was dried at 110 °C and allowed to cool in a vacuum desiccator prior to making the pellets, to avoid adsorption of moisture. All IR spectra of samples were recorded in the range 400–4000 cm^{-1} using the following settings: number of scans 4; gain 1; apodization weak; OPD velocity 0.3 cm/s; and resolution 4.

3. Results and discussion

3.1. X-ray diffraction

The amorphous nature of the samples was confirmed from X-ray diffraction. XRD patterns for the glasses are shown in Fig. 1. The XRD pattern of V₂O₅ polycrystalline powder has 3 strongest peaks at $2\theta = 20.3^\circ$, 26.1° and 31° with intensities 100%, 75% and 52%, respectively. Fig. 1 exhibits a broad diffuse scattering at low angles instead of crystalline peaks confirming a long-range structural disorder characteristic of amorphous network, i.e., XRD patterns indicated glassy behavior with a broad hump at $2\theta = 25\text{--}27^\circ$ with the observation of no peak corresponding to V₂O₅ indicating that V₂O₅ has completely entered the glass matrix and that the glasses formed were completely amorphous.

3.2. FT-IR spectra

Although infrared spectra were recorded in the wider range 400–4000 cm^{-1} , the range 400–2000 cm^{-1} for all glasses was selected and shown in Fig. 1 and Table 2. This is the fingerprinting range of primary interest as no significant changes are observed beyond 2000 cm^{-1} and also spectra from 2000 cm^{-1} towards higher numbers look the same for all compositions. For comparison, spectra are also shown for V₂O₅, SrO and B₂O₃ in Fig. 1 and Table 2.

3.2.1. IR for pure B₂O₃

The transmission peaks observed for B₂O₃ are shown in Fig. 2 and Table 2 as follows: 1505–1352 cm^{-1} (broad peak)

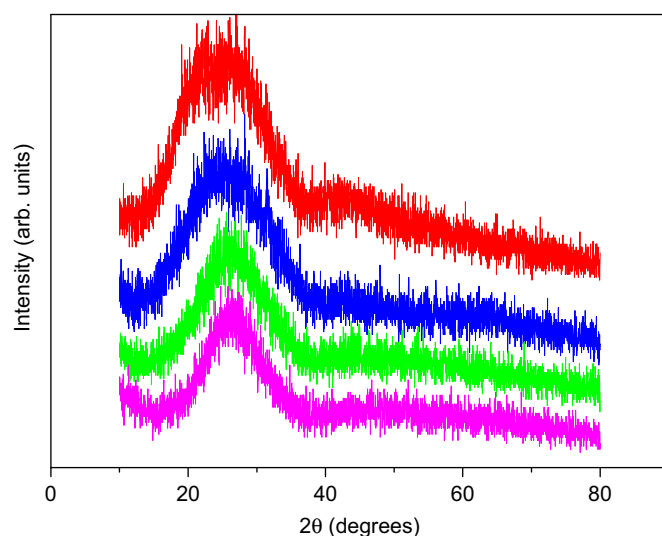


Fig. 1. XRD for different glass composition of SrO-borovanadate $(V_2O_5)_{0.5}(SrO)_{0.5-y}(B_2O_3)_y$ glasses at room temperature.

Table 2

Characteristic infrared absorptions peaks (cm^{-1}) for V_2O_5 , B_2O_3 , SrO, and SrO-borovanadate glasses $(\text{V}_2\text{O}_5)_{0.5}(\text{SrO})_{0.5-y}(\text{B}_2\text{O}_3)_y$

V_2O_5	1502s	1190s	1019 mp	845–805 bp	594–473 small peaks
SrO	1699	1458	1026	855	450–409 Small peaks
B_2O_3	1505–1352 bp	1453sh	1037sh and 1008 sp	806–771 bp	600–585 broad
$y = 0.0$	1552–1500 sh or s	1451sh	948 sp	890 bp	646–467 small peaks
$y = 0.1$	1555–1536 Sh or s	1384–1297bp		886 bp	454–400bs
$y = 0.2$	1554–1525 s	SAME		886 bp	
$y = 0.3$	1534 sh	SAME		
$y = 0.4$	1550 sh	SAME		
		1200 only	980sh	
			990sp	

s (small), sp (sharp peaks), mp (main peak), bp (broad peak), ob (obvious but small), sh (shoulder), bs (bunch of small peaks).

1190–1137 cm^{-1} (small peaks but sharp), 1008–948 cm^{-1} (sharp peaks), 806–771 cm^{-1} (broad peak), and a sharp peak at 694 cm^{-1} . There are small peaks in the region 646–467 cm^{-1} . The presented IR spectrum for B_2O_3 shows quite a good match with that reported in the literature [9].

3.2.2. IR for pure V_2O_5

As seen from Fig. 2, peaks were recorded at 1019 cm^{-1} (main peak used in the discussion), 845–805 cm^{-1} (broad peak), broad band from 594 to 470 cm^{-1} together with small bumps at 1502 and 1190 cm^{-1} . Our data agree quite well with that shown in Ref. [13], where peaks have been observed at 1020, 810, 600 and 480 cm^{-1} .

3.2.3. IR for pure SrO

For SrO powder, peaks were recorded at 1699, 1458, 1026 and 855 cm^{-1} with broad bands from 585 to 600 cm^{-1} and 409 to 450 cm^{-1} as shown in Table 2.

3.2.4. Main features of IR spectra for Sr-borovanadate glasses

$(\text{V}_2\text{O}_5)_{0.5}(\text{SrO})_{0.5-y}(\text{B}_2\text{O}_3)_y$

Infrared spectra studies have been carried out on powdered samples dispersed in KBr pellets and shown in Fig. 2 for the range 400–2000 cm^{-1} . For all glasses, water band around 3400 cm^{-1} and –OH stretching peaks around 2400 were observed. A peak was observed at 1646 cm^{-1} for all glasses and is independent of the concentration of the constituents of the glasses. The origin of these peaks is not obvious, but the –OH bending mode gives rise to absorption in this region and the possibility of some adsorbed water giving rise to these peaks cannot be ruled out. Hence, the bands observed in the range 1600–3400 cm^{-1} are possibly due to the hygroscopic nature of powdered samples. Further, these bands are obtained in all the glasses almost at the same position.

The strong band observed for V_2O_5 at 1019 cm^{-1} , which was reported at 1020 cm^{-1} by previous studies [14], carried out on SrO-vanadate glasses, has been assigned to the vibration of the isolated $\text{V}=\text{O}$ non-bridge bonds in the VO_5 trigonal bipyramids [15]. With the addition of SrO, changes are observed in the spectra. In the case of SrO-vanadate glasses with SrO content 20–30%, a band at 968 cm^{-1} is observed with reduced intensity in the spectra (a shoulder is also observed at 968 cm^{-1} for SrO content 40%) and for glasses with SrO content 30%, 40% and 50% a band at 886 cm^{-1} is observed but this band is missing from IR spectrum for glass containing 20% SrO [16]. Further, it is observed that the band around 1020 cm^{-1} completely vanishes for these glasses, suggesting that the isolated $\text{V}=\text{O}$ bonds might have vanished or become too weak to be detected.

The IR spectra for SrO-borovanadate glasses arise largely from the modified borate networks. According to previous studies [17], the structure of boron oxide glass consists of a random network of planer BO_3 triangles with a certain fraction of six-membered (boroxol) rings. X-ray and neutron diffraction data suggest that glass structure consists of a random network of BO_3 triangles without boroxol rings. By looking at the IR spectra (Fig. 2 and Table 2), the vibrational modes of the borate network are seen to be active in four IR spectral regions, which are similar to those previously reported [18].

- The first group of bands that occurs from 1200 to 1600 cm^{-1} is due to the asymmetric stretching–relaxation of the B–O bond of triangle BO_3 units.
- The second group lies between 900 and 1200 cm^{-1} and is due to B–O bond stretching of the tetrahedral BO_4 units.
- The third group is around 800 and 900 cm^{-1} and is due to the bending of B–O–B linkages in borate networks.
- Below 800, there are several peaks in B_2O_3 , V_2O_5 and SrO and are retained in all these glasses.

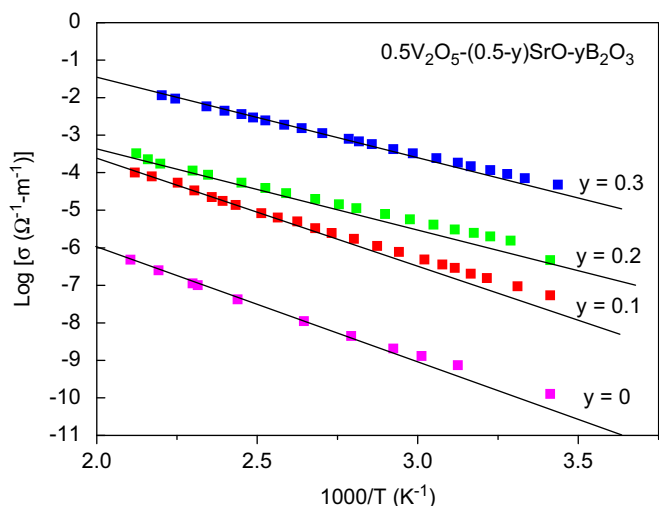


Fig. 3. Temperature dependence of dc conductivity, σ for SrO-borovanadate $(V_2O_5)_{0.5}(SrO)_{0.5-y}(B_2O_3)_y$ glasses as plots of $\text{Log } \sigma$ as a function of $1000/T$. The solid lines are the least-square fits to the data.

Table 3

Activation energy W (eV) and $\text{Log } \sigma(\Omega\text{-m})^{-1}$ at 400 K for SrO-borovanadate glasses $(V_2O_5)_{0.5}(SrO)_{0.5-y}(B_2O_3)_y$.

Nominal	W (eV)	$\text{Log } \sigma(\Omega\text{-m})^{-1}$	T_{cal} (K) ^a	NBO/ T_{O}^b	$V_{4+}/V_{\text{total}}^b$
$y = 0.0$	0.59	-7.539	230	1.00	0.0206
$y = 0.1$	0.57	-5.069		0.891	0.0225
$y = 0.2$	0.44	-4.42		0.751	0.0270
$y = 0.3$	0.39	-2.252		0.649	0.0276
				0.619	0.0204

^a Theoretical slope ($\tan \theta = -1/2.303 k_B T$).

^b From reference (Khattak et al. Phys. Rev. B).

The values of ‘ W ’ were calculated by fitting the experimental data to the equation

$$\text{Log } \sigma = \text{Log } \sigma_0 - (W/1000 k_B T)(1000/T)(1/2.303) \quad (2)$$

The activation energy W (eV) and the values of $\text{Log } \sigma (\Omega\text{ m})^{-1}$ at 400 K are shown in Table 3 for SrO-borovanadate glasses. Mostly, studies have been concerned with the dependence of electrical conductivity on V_2O_5 content and the V^{4+}/V^{5+} ratio. In their study of the electrical properties of glasses of the systems $\text{CaO-B}_2\text{O}_3\text{-V}_2\text{O}_5$ and $\text{CaO-P}_2\text{O}_5\text{-V}_2\text{O}_5$, Kennedy and Mackenzie [23] indicated that for similar compositions and similar V^{4+}/V^{5+} ratios, the conductivity of borate glasses is lower than that of phosphate glasses. They deduced that the network former has a great effect on the electrical conduction of such glasses. Generally, it is known that ionic conductivity increases as a result of breakdown of bridging oxygen (BO) bonds and formation of non-bridging oxygen ions [24]. This produces the so-called open structure, through which the charge carriers can move with higher mobility. In our case, it is observed that $\text{NBO}/O_{\text{total}}$ decreases while both dc conductivity and the ratio V^{4+}/V_{total} increase with increase in the content of B_2O_3 [22, Table 3]. Hence, the bridging oxygen (BO) bonds are strengthened, which indicates that the conductivity depends on the ratio of V^{4+}/V_{total} , and hence the presence of electronic conductivity.

In Mott’s model [25,26] for conduction process in TMO glasses, the conduction mechanism is considered in terms of phonon-assisted hopping of small polarons between localized states. According to this model, DC conductivity for the nearest-

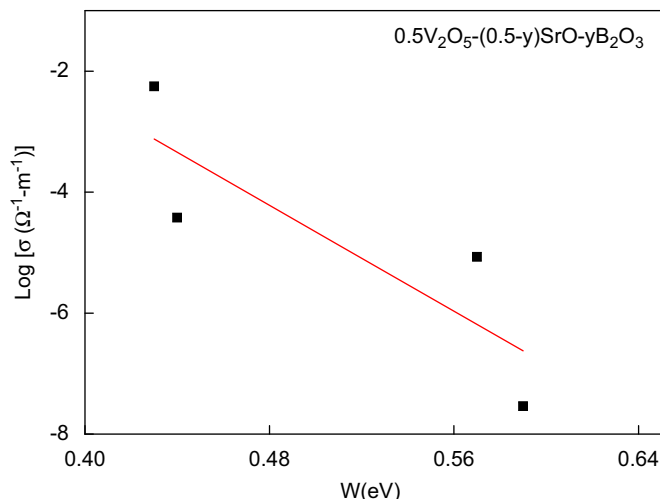


Fig. 4. A plot of $\text{Log } \sigma$ versus W for SrO-borovanadate $(V_2O_5)_{0.5}(SrO)_{0.5-y}(B_2O_3)_y$ glasses at 400 K.

neighbor hopping in non-adiabatic regime at high temperatures ($T \gg \theta_D/2$) is given by

$$\sigma = v_o N e^2 R^2 / k_B T C (1 - C) \exp(-2\alpha R) \exp(-W/k_B T) \quad (3)$$

where v_o is the longitudinal optical phonon frequency, C the fraction of reduced vanadium ions, V^{4+}/V_{total} , α^{-1} the localization length for the wave function, R the average hopping distance, k_B the Boltzmann constant, e the electronic charge and w the activation energy for hopping conduction.

The activation energy for hopping conduction is given by [5]

$$W = W_D + W_H/2, \quad \text{for } T > \theta_D/2$$

$$W \approx W_D, \quad \text{for } T < \theta_D/4$$

where W_H is the hopping energy, W_D the energy difference between two adjacent sites, i.e., disorder energy and θ_D is the Debye temperature.

In the framework of Mott’s model, the nature of the polaron hopping mechanism in the high-temperature range (adiabatic or non-adiabatic), where an activated behavior of conductivity was observed, can be ascertained from the plot $\text{Log } \sigma$ versus activation energy, W , at an arbitrary experimental temperature in this range. It has been suggested [26,27] that the hopping would be in the adiabatic regime if the temperature estimated, T_c , from the slope of such a plot were close to the experimental temperature T . Otherwise, the hopping would be in the non-adiabatic regime. A plot of $\text{Log } \sigma$ at 400 K versus W is shown in Fig. 4 for these glasses. It is evident from the figure that the data are very scattered but we have tried to fit the data into a straight line. The temperature calculated, T_c , from the fitted line is very different from the experimental temperature chosen (400 K) (Table 3), suggesting that the conduction mechanism in the present glasses is due to non-adiabatic hopping of the polarons [25,26] (see Fig. 5).

The experimental results were analyzed with reference to theoretical models existing in the literature.

3.3.1. Greaves law of variable range hopping (VRH)

According to this model [28], the expression for conductivity can be written as

$$\sigma T^{1/2} = A \text{Exp}(-B/T^{1/4}) \quad (4)$$

where A and B are constants. The values of A and B can be obtained from the intercept and slope, respectively, of the plot $\text{Log}(\sigma T^{1/2})$

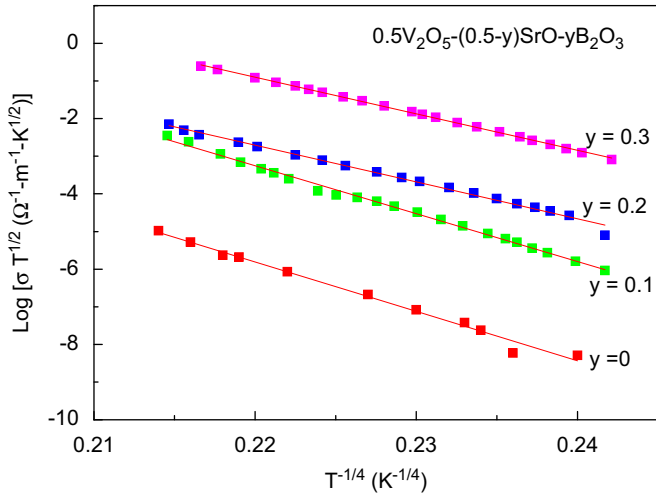


Fig. 5. A plot of $\text{Log}(\sigma T^{1/2})$ versus $T^{-1/4}$ for SrO-borovanadate $(\text{V}_2\text{O}_5)_{0.5}(\text{SrO})_{0.5-y}(\text{B}_2\text{O}_3)_y$ glasses. The solid lines are the best fits to Eq. (4).

Table 4

Parameters A , B , N_C obtained for Greaves variable-range hopping conduction^a for SrO-borovanadate glasses $(\text{V}_2\text{O}_5)_{0.5}(\text{SrO})_{0.5-y}(\text{B}_2\text{O}_3)_y$, $\alpha = 33 \text{ nm}^{-1}$.

Nominal	$\text{Log} A [(\Omega\text{-m})^{-1} \text{K}^{1/2}]$	$B (\text{K}^{1/4})/2.303$	$N_C (\times 10^{21} \text{ eV}^{-1}/\text{cm}^3)$
$y = 0.0$	23.053	129.479	0.97
$y = 0.1$	24.732	121.004	1.10
$y = 0.2$	18.809	93.978	3.15
$y = 0.3$	20.492	93.446	3.22

$$^a \sigma T^{1/2} = A \exp(-B/T^{1/4}) N_C = (2.882 \times 10^{29})/(\text{slope})^4 \text{ eV}^{-1}/\text{cm}^3.$$

versus $T^{-1/4}$. Further, the value of B can be written as

$$B = 2.1[\alpha^3/k_B N_C]^{1/4} \quad (5)$$

Fig. 5 shows the plots of $\text{Log}(\sigma T^{1/2})$ versus $T^{-1/4}$ and the linear relationship confirms the Greaves VRH model [28]. The values of parameters A and B obtained from these curves are given in Table 4. Values of the density of states at the Fermi level, N_C , were estimated from Eq. (5) assuming $\alpha = 33 \text{ nm}^{-1}$ [29] and shown in Table 4. These values are consistent with those of the usual semiconducting oxide glasses [30,31], suggesting that this model is suitable to explain the conductivity data. Thus, it is concluded that the appearance of the VRH for the temperature interval of measurements, $T = 293\text{--}470 \text{ K}$, is reasonable for the present glasses.

3.3.2. Schnakenberg's polaron hopping model

A polaron hopping model, where $W_D \neq 0$, has been considered by Schnakenberg [32]. In this model, the optical multiphonon hopping process determines dc conductivity at high temperature, while at low temperatures the conductivity is determined by the acoustical single-phonon-assisted hopping process. In this model, the expression for dc conductivity as a function of temperature is given by

$$\sigma = A/T[\sinh(h\nu_0/k_B T)]^{1/2} \text{Exp}[-(4W_H/h\nu_0) \tan h(h\nu_0/4k_B T)] \times \text{Exp}(-W_D/k_B T) \quad (6)$$

Eq. (6) predicts a temperature-dependent hopping energy which decreases with increase in temperature, consistent with the data presented in Fig. 3. Fig. 6 shows plots of $\text{Log}(\sigma T)$ versus

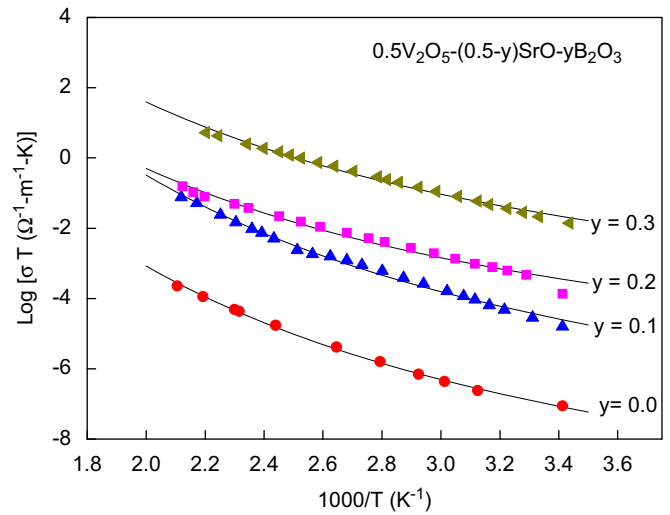


Fig. 6. Best fits (solid curves) of the Schnakenberg model Eq. (6) to the experimental data for SrO-borovanadate $(\text{V}_2\text{O}_5)_{0.5}(\text{SrO})_{0.5-y}(\text{B}_2\text{O}_3)_y$ glasses as plots of $\text{Log}(\sigma T)$ versus $1000/T$.

Table 5

Parameters obtained by fitting the dc conductivity data to the Schnakenberg model for SrO-borovanadate glasses $(\text{V}_2\text{O}_5)_{0.5}(\text{SrO})_{0.5-y}(\text{B}_2\text{O}_3)_y$.

Nominal	$\nu_0 \times 10^{13} (\text{s}^{-1})$	$W_H (\text{eV})$	$W_D (\text{eV})$	$W_H+W_D/2 (\text{eV})$
$y = 0.0$	0.99	0.48	0.02	0.49
$y = 0.1$	1.9	0.77	0.04	0.79
$y = 0.2$	2.1	0.73	0.04	0.75
$y = 0.3$	2.8	0.84	0.05	0.87

$1000/T$ and the DC conductivity has been fitted to the theoretical values given by this model (Eq. (6)). W_H , W_D and ν_0 were used as variable parameters in the fitting process and the best fits of the data have been obtained for the values of the parameters shown in Table 5. The values of ν_0 are close to the values previously reported [29]. However, this model yields high values of W_H than the values of the activation energy estimated for the temperature range of measurements (Table 2). Further, $W_H+W_D/2$ is not equal to W (Table 3) and so is not in accordance with the prediction of the Mott model [25,26].

3.3.3. Mott's model

At low temperatures, where polaron binding energy is very small and disorder energy, W_D , plays a dominant role in the conduction mechanism, Mott and Davis [33] have shown that hops may occur preferentially beyond nearest neighbors. The conductivity for the so-called variable range hopping mechanism is given by

$$\sigma = B \text{Exp}(-A/T^{1/4}) \quad (7)$$

where

$$A = 4[2\alpha^3/9\pi k_B N(E_F)]^{1/4} \quad (8)$$

$$B = [e^2/2(8\pi)^{1/2}] \nu_0 [N(E_F)/\alpha k_B T]^{1/2} \quad (9)$$

and α is the decay of the localized state wavefunction, and $N(E_F)$ the density of state at the Fermi level. Fig. 7 shows plots of $\text{Log} \sigma$ versus $T^{-1/4}$ and it is observed that the plots are linear over almost the whole temperature range of measurements consistent with the Mott VRH model. Eq. (7) was fitted to the experimental data and the values of A and B calculated from these fits are given

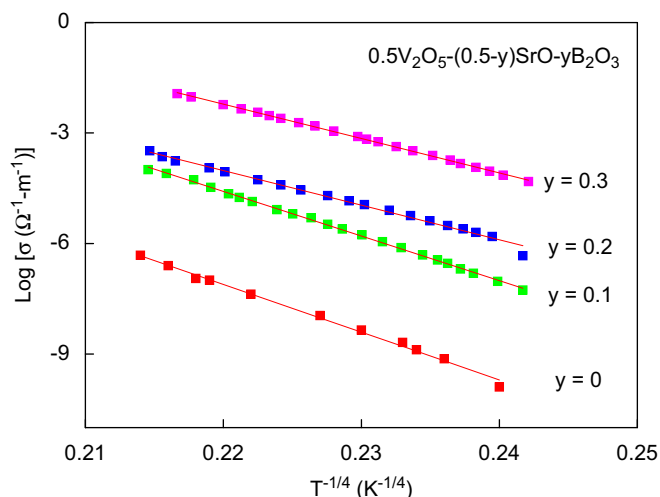


Fig. 7. A plot of $\text{Log } \sigma$ versus $T^{-1/4}$ for SrO-borovanadate $(\text{V}_2\text{O}_5)_{0.5}(\text{SrO})_{0.5-y}(\text{B}_2\text{O}_3)_y$ glasses. The solid lines are best fits to Eq. (7).

Table 6

Parameters A , B , $N(E_F)$ obtained for Mott's variable-range hopping and percolation model^a for Sr-borovanadate glasses $(\text{V}_2\text{O}_5)_{0.5}(\text{SrO})_{0.5-y}(\text{B}_2\text{O}_3)_y$.

Nominal	A ($\text{K}^{1/4}$) / 2.303	$\text{Log } B$ [$(\Omega\text{-m})^{-1}$]	$N(E_F)$ ($\times 10^{21}\text{-eV}^{-1}\text{cm}^{-3}$)
$y = 0.0$	129.479	21.374	0.953
$y = 0.1$	121.004	22.034	1.25
$y = 0.2$	93.978	16.655	3.44
$y = 0.3$	93.446	18.343	3.52

$\alpha = 33\text{ nm}^{-1}$.

$$^a \sigma = B \exp(-A/T^{1/4}) N(E_F) = 2.68 \times 10^{29} / (\text{slope})^4 \text{ eV}^{-1} \text{ cm}^{-3}.$$

in Table 6. Assuming a reasonable value of $\alpha^{-1} \approx 10\text{ \AA}$, values of $N(E_F)$ were calculated from Eq. (8). These values, shown in Table 6, are comparable with the values obtained for the vanadate glasses formed with traditional network former and the other semiconducting glasses [33–36].

4. Conclusions

The overall features of XRD patterns confirm the amorphous nature of the present glasses. The IR results agree with previous investigations on similar glasses and it has been hypothesized that with the introduction of B_2O_3 into SrO-vanadate glasses, B atoms would substitute into V sites of various VO_n polyhedra and not result in any additional structural units. On B_2O_3 concentration exceeding the SrO content, a third grouping is realized as BO_n structures, such as metaborate chain structures, BO_4 polyhedra or $\text{Sr}_2\text{B}_2\text{O}_5$ units are formed in boron-rich regions in the borovanadate glass network in addition to VO_n polyhedra and SrV_2O_6 structures. Thus, this qualitative picture of the local glass structure evolving as the relative concentration varies in these SrO-vanadate and SrO-borovanadate glasses is very similar to the interpretation of the glass structure based on the previous IR and EXFAS studies on

these glasses. The temperature dependence of DC electrical conductivity of SrO-vanadate and SrO-borovanadate glasses has been studied in terms of different hopping models. The data suggest that the conduction mechanism in the present glasses is due to non-adiabatic hopping of polarons. Further, analysis of the conductivity data shows that the conductivity data are consistent with Mott's nearest neighbor hopping model. However, both Mott VRH and Greaves models are suitable to explain the data. Schnakenberg's generalized polaron hopping model is consistent with the temperature dependence of the activation energy. However, the various model parameters such as density of states, hopping energy, etc., obtained from the best fits were not found to be in accordance with the prediction of the Mott model [3].

Acknowledgement

The support of the KFUPM Physics Department and Research Committee (Grant # Ph/Glasses/346) is greatly acknowledged.

References

- [1] G.S. Linsley, A.E. Owen, F.M. Hayatee, *J. Non-Cryst. Solids* 4 (1970) 208.
- [2] A.W. Dozier, L.K. Wilson, E.J. Friebel, D.L. Kinser, *J. Am. Ceram. Soc.* 55 (1972) 373.
- [3] B.S. Rawal, R.K. Maccrone, *J. Non-Cryst. Solids* 28 (1978) 347.
- [4] N.F. Mott, *J. Non-Cryst. Solids* 1 (1968) 1.
- [5] I.G. Austine, N.F. Mott, *Adv. Phys.* 18 (1969) 45.
- [6] S. Sen, A. Ghosh, *J. Mater. Res.* 15 (2000) 995.
- [7] S. Sen, A. Ghosh, *J. Non-Cryst. Solids* 258 (1999) 29.
- [8] S. Sindhu, S. Sanghi, A. Agarwal, Sonam, V.P. Seth, N. Kishore, *Physica B* 365 (2005) 65.
- [9] B.K. Sharma, D.C. Dube, Abhai Mansingh, *J. Non-Cryst. Solids* 65 (1984) 39.
- [10] A. Ghosh, *J. Appl. Phys.* 64 (1988) 2652.
- [11] R.A. Montani, M. Levy, J.L. Souquet, *J. Non-Cryst. Solids* 149 (1992) 249.
- [12] A. Ghosh, B.K. Chaudhuri, *J. Non-Cryst. Solids* 103 (1988) 83.
- [13] Y. hakamatsuka, N. Yoneda, T. Tsuchiya, *Yogyo Kyokai Shi* 90 (1962) 48.
- [14] V. Dimitrov, Y. Dimitriev, M. Arnaudov, D. Topalov, *J. Non-Cryst. Solids* 57 (1983) 147.
- [15] E. Dacheille, R. Roy, *J. Am. Ceram. Soc.* 42 (1965) 78.
- [16] G.D. Khattak, A. Mekki, to be published.
- [17] M.J. Krogh, *J. Phys. Chem. Glasses* 6 (1965) 46.
- [18] E.I. Kamitsos, M.A. Karakassides, G.D. Chryssikos, *J. Phys. Chem. Glasses* 91 (1987) 1073.
- [19] T. Hubert, G. Mosel, K. Witke, *Glass Phys. Chem.* 27 (2001) 114.
- [20] O. Attos, M. Massot, M. Balkanski, E. Haro-Poniatowski, M. Asomoza, *J. Non-Cryst. Solids* 210 (1997) 163.
- [21] T. Hubert, U. Harder, G. Mosel, K. Witke, in: A.C. Wright, S.A. Feller, A.C. Hannon (Eds.), *Borate Glasses, Crystals, and Melts II*, Society of Glass Technology, Sheffield, 1997, p. 156.
- [22] G.D. Khattak, N. Tabet, L.E. Wenger, *Phys. Rev. B* 72 (2005) 104203.
- [23] T.N. Kennedy, J.D. Mackenzie, *Phys. Chem. Glasses* 8 (1967) 169.
- [24] A.E. Owen, *Progress in Ceramic Science*, vol. 3. Pergamon, Oxford, p. 350.
- [25] N.F. Mott, *Philos. Mag.* 19 (1969) 835.
- [26] M. Sayer, A. Mansingh, *Phys. Rev. B* 6 (1972) 4629.
- [27] C.H. Chung, J.D. Mackenzie, L. Murawski, *Rev. Chem. Miner.* 16 (1979) 308.
- [28] G.N. Greaves, *J. Non-Cryst. Solids* 11 (1973) 427.
- [29] S. Sen, A. Ghosh, *J. Phys.: Condens. Matter* 11 (1999) 1529.
- [30] M.M. El-Desoky, Kashif, *Phys. Status Solidi (a)* 194 (2002) 89.
- [31] A. Al-Shahrani, A. Al-Hajri, M.M. El-Desoky, *Phys. Status Solidi (a)* 300 (2003) 378.
- [32] J. Schnakenberg, *Phys. Status Solidi* 28 (1968) 623.
- [33] N.F. Mott, E.A. Davis, *Electronic Processes in Non-Crystalline Materials*, second ed., Clarendon, Oxford, 1979.
- [34] A. Ghosh, *Phys. Rev. B* 42 (1990) 5665.
- [35] A. Ghosh, *J. Appl. Phys.* 66 (1989) 2425.
- [36] A. Ghosh, *J. Chem. Phys.* 102 (1995) 1385.